We amplified a sequence demonstrating complete identity to the homologous 590-bp segment of the *omp*A gene of *R. parkeri* strain Maculatum 20 (GenBank accession no. U43802) from 1 (7%) of 14 ticks collected in 2016. We further amplified sequences demonstrating complete identities to the homologous segments of the *ompA* (590 bp) and 17-kDa antigen (208 bp) genes of *Candidatus* Rickettsia andeanae (GenBank accession nos. KF179352 and KY402193, respectively) from another tick in this group and sequences revealing complete identity to each other and to the homologous segments of the *glt*A (760 bp), *omp*B (760 bp), and *omp*A (490 bp) genes of *R. parkeri* strain Portsmouth (GenBank accession no. CP003341.1) from 10 (71%) of 14 ticks evaluated from the 2017 collection.

We identified DNA of *R. parkeri* and *Candidatus* Rickettsia andeanae in *A. maculatum* group ticks in northern Sonora. *R. parkeri* causes a disease less severe than RMSF and should be suspected in patients with an eschar, rash, and lymphadenopathy (*1*). The results of this investigation suggest that *R. parkeri* could contribute to at least some of the cases of spotted fever rickettsiosis described in Sonora and possibly in other regions of Mexico where *A. maculatum* group ticks are found. Differentiation between these 2 diseases is important, principally because there are no reports of fatal disease caused by *R. parkeri.* Nonetheless, clinical suspicion of any SFGR requires immediate treatment with doxycycline. *Candidatus* Rickettsia andeanae, a SFGR of undetermined pathogenicity, has been detected in the United States and Central and South America (*2,10*). Our findings highlight the need for specific diagnostic tests for SFGR in Mexico that can identify other potential SFGR of public health concern in this country.

About the Author

Dr. Delgado-de la Mora is a researcher and resident of Pathology at Instituto Nacional de Ciencias Médicas y Nutrición Salvador Zubirán. His research interests include tickborne diseases, particularly those caused by *Rickettsia* spp.

References

1. Paddock CD, Sumner JW, Comer JA, Zaki SR, Goldsmith CS, Goddard J, et al. *Rickettsia parkeri*: a newly recognized cause of spotted fever rickettsiosis in the United States. Clin Infect Dis. 2004;38:805–11. http://dx.doi.org/10.1086/381894
2. Allerdice MEJ, Beati L, Yaglom H, Lash RR, Delgado-de la Mora J, Licona-Enriquez JD, et al. *Rickettsia parkeri* (Rickettsiales: Rickettsiaceae) detected in ticks of the *Amblyomma maculatum* (Acari: Ixodidae) group collected from multiple locations in southern Arizona. J Med Entomol. 2017;54:1743–9. http://dx.doi.org/10.1093/jme/tjx138
3. Álvarez-Hernández G, Roldán JFG, Milan NSH, Lash RR, Behravesh CB, Paddock CD. Rocky Mountain spotted fever in Mexico: past, present, and future. Lancet Infect Dis. 2017;17:e189–96. http://dx.doi.org/10.1016/S1473-3099(17)30173-1
4. Sánchez-Montes S, López-Pérez AM, Guzmán-Cornejo C, Colunga-Salas P, Becker I, Delgado-de la Mora J, et al. *Rickettsia parkeri* in *Dermacentor parumapertus* ticks, Mexico. Emerg Infect Dis. 2018;24:1108–11. http://dx.doi.org/10.3201/eid2406.180058
5. Lado P, Nava S. Mendoza-Uribe L, Caceres AG, Delgado-de la Mora J, Lincona-Enriquez JD, et al. The *Amblyomma maculatum* Koch, 1844 (Acari: Ixodidae) group of ticks: phenotypic plasticity or incipient speciation? Parasites Vectors. 2018;11:610.
6. Kato CY, Chung IH, Robinson LK, Austin AL, Dasch GA, Massung RF. Assessment of real-time PCR assay for detection of *Rickettsia* spp. and *Rickettsia rickettsii* in banked clinical samples. J Clin Microbiol. 2013;51:314–7. http://dx.doi.org/10.1128/JCM.01723-12
7. Regnery RL, Spruill CL, Plikaytis BD. Genotypic identification of rickettsiae and estimation of intraspecies sequence divergence for portions of two rickettsial genes. J Bacteriol. 1991;173:1576–89. http://dx.doi.org/10.1128/jb.173.5.1576-1589.1991
8. Massung RF, Davis LE, Slater K, McKechnie DB, Puerzer M. Epidemic typhus meningitis in the southwestern United States. Clin Infect Dis. 2001;32:979–82. http://dx.doi.org/10.1086/319351
9. Tzianabos T, Anderson BE, McDade JE. Detection of *Rickettsia rickettsii* DNA in clinical specimens by using polymerase chain reaction technology. J Clin Microbiol. 1989;27:2866–8.
10. Paddock CD, Fournier PE, Sumner JW, Goddard J, Elshenawy Y, Metcalfe MG, et al. Isolation of *Rickettsia parkeri* and identification of a novel spotted fever group *Rickettsia* sp. from Gulf Coast ticks (*Amblyomma maculatum*) in the United States. Appl Environ Microbiol. 2010;76:2689–96. http://dx.doi.org/10.1128/AEM.02737-09

Address for correpondence: Jesús Delgado-de la Mora, Instituto Nacional de Ciencias Médicas y Nutrición Salvador Zubirán, Departamento de Anatomía Patológica, Avenida Vasco de Quiroga 15, Belisario Domínguez, C.P. 14080, Mexico City, Mexico; email: jdelgadom1992@gmail.com

Reduced Susceptibility to Neuraminidase Inhibitors in Influenza B Isolate, Canada

Yacine Abed,[1] Clément Fage,[1] Patrick Lagüe, Julie Carbonneau, Jesse Papenburg, Donald C. Vinh, Guy Boivin

Author affiliations: Laval University, Québec City, Québec, Canada (Y. Abed, C. Fage, P. Lagüe, J. Carbonneau, G. Boivin); Montreal Children's Hospital, Montreal, Québec (J. Papenburg); McGill University Health Center, Montreal (D.C. Vinh)

DOI: https://doi.org/10.3201/eid2504.181554

[1]These authors contributed equally to this article.

We identified an influenza B isolate harboring a Gly407Ser neuraminidase substitution in an immunocompromised patient in Canada before antiviral therapy. This mutation mediated reduced susceptibility to oseltamivir, zanamivir, and peramivir, most likely by preventing interaction with the catalytic Arg374 residue. The potential emergence of such variants emphasizes the need for new antivirals.

Neuraminidase inhibitors (NAIs) are recommended for the control of severe influenza A and B infections (*1*). Nevertheless, antiviral resistance may emerge in immunocompromised persons, with major clinical implications (*2*).

In 2017–18, influenza B/Yamagata/16/88-like strains accounted for 50% of seasonal infections in Canada (*3*). In March 2018, we identified an influenza B/Yamagata/16/88–like variant containing a Gly407Ser NA substitution conferring reduced susceptibility to various NAIs. This variant was recovered from an immunocompromised patient before NAI therapy.

The 62-year-old woman, who had non-Hodgkin lymphoma, underwent an autologous stem cell transplant in February 2017. In March 2018, she developed therapy-related acute myeloid leukemia that failed to respond to cytarabine treatment. During hospitalization, she had influenza-like symptoms, with confirmed influenza B detection by RT-PCR. Oseltamivir (75 mg 2×/d) was administered during March 27, 2018–April 4, 2018. Because the patient's respiratory symptoms worsened and influenza B persisted despite treatment, we replaced oseltamivir with intravenous zanamivir (600 mg 2×/d) but switched back to oseltamivir because of respiratory distress episodes. Ultimately, the patient opted to stop treatment and died a few days later.

We sequenced the viral hemagglutinin (HA) and NA genes from nasopharyngeal swab specimens using the ABI 3730 analyzer (Thermo Fisher, https://www.thermofisher.com). The HA (GenBank accession no. MH450013) and NA (GenBank accession no. MH449670) sequences from the March 27, 2018, specimen (pretherapy: B/Quebec/1182C/2018) were identical to the April 4, 2018, specimen (day 9 of oseltamivir therapy), sharing 99.5% aa identity with the HA (GenBank accession no. EPI544262) and 98.7% with the NA (GenBank accession no. EPI544263) of the B/Phuket/3073/2013 vaccine strain. Both clinical samples contained a Gly407Ser NA substitution, a marker of NAI resistance (*4*). We cloned the NA gene from pre– and post–oseltamivir therapy viruses into pJET cloning plasmid and sequenced 15 clones per virus. All NA clones contained the Gly407Ser mutation.

We used an unrelated 2018 isolate (B/Quebec/88855/2018; GenBank accession nos. MH450019 for HA, MH450017 for NA) as a wild-type control for further in vitro characterization. B/Quebec/88855/2018 (wild-type) and B/Quebec/1182C/2018 (Gly407Ser) shared 99.8% aa HA and 99.4% aa NA identities.

We determined NAI 50% inhibitory concentrations (IC_{50}s) of isolates using fluorometric-based NA inhibition assays (*5*) and evaluated their NA activity (V_{max} [maximum velocity of substrate conversion]) by performing enzyme kinetics experiments (*6*). B/Quebec/1182C/2018 demonstrated reduced inhibition (RI; 5- to 50-fold increases in IC_{50} over wild-type) (*4*) to oseltamivir, zanamivir, and peramivir, showing 5.97-, 32.44-, and 38.34-fold increases in IC_{50}s, respectively, over B/Quebec/88855/2018 WT (Table). The last 2 isolates had similar NA activity (V_{max}) (Table). To confirm the role of the Gly407Ser mutation, we expressed the recombinant wild-type and Gly407Ser mutant proteins (obtained by PCR-mediated mutagenesis) in 293T cells (*7*) and found that Gly407Ser also increased oseltamivir, zanamivir, and peramivir IC_{50}levels by 4.16-, 10.07- and 16.36-fold, respectively (Table).

We next evaluated replication kinetics of the wild-type and Gly407Ser isolates in ST6GalI-MDCK cells. Mean viral titers obtained with wild-type isolates were higher than the mutant at 24 and 48 h postinfection ($p<0.01$); comparable titers were obtained at 72 and 96 h postinfection (Appendix Figure 1, http://wwwnc.cdc.gov/EID/article/25/4/18-1554-App1.pdf). To assess genetic stability, we sequenced the HA/NA genes after 4 passages in

Table. Susceptibility profiles and NA activity of influenza B virus isolates and susceptibility profiles of recombinant influenza B NAs determined by assays using the fluorescent MUNANA substrate, Canada*

Sample type	IC_{50} in nM ± SD (fold increase) [phenotype]†			NA activity, V_{max}‡
	Oseltamivir	Zanamivir	Peramivir	
Clinical isolate				
B/Phuket/3073/2013, vaccine	18.98 ± 3.89	0.70 ± 0.17	0.74 ± 0.02	ND
B/Québec/88855/2018, WT	17.47 ± 1.43 (1) [NI]	0.85 ± 0.09 (1) [NI]	0.92 ± 0.09 (1) [NI]	2.24 ± 0.3
B/Québec/1182C/2018, Gly407Ser	104 ± 14.62 (5.97) [RI]	27.58 ± 2.56 (32.44) [RI]	26.08 ± 0.1 (38.34) [RI]	2.18 ± 0.47
Recombinant neuraminidase				
B/Quebec/88855/2018, WT	11.16 ± 5.25 (1) [NI]	0.97 ± 0.27 (1) [NI]	0.76 ± 0.19 (1) [NI]	ND
B/Quebec/88855/2018, Gly407Ser	46.52 ± 12.58 (4.16) [NI]	9.77 ± 0.90 (10.07) [RI]	12.44 ± 5.47 (16.36) [RI]	ND

*Values are from a representative experiment performed in duplicate. IC_{50}, 50% inhibitory concentration; MUNANA, 2 '-(4-methylumbelliferyl)-α-D-N-acteylneuraminic acid; NA, neuraminidase; NAI, neuraminidase inhibitor; ND, not done; NI, normal inhibition (<5-fold increase in IC_{50} over WT); RI, reduced inhibition (5- to 50-fold increase in IC_{50} over WT); V_{max}, maximum velocity of substrate conversion; WT, wild type.
†The phenotype of susceptibility to NAI following the World Health Organization guidelines.
‡Numbers indicate mean V_{max} values (U/sec) ± SD of a kinetics experiment performed in triplicate.

ST6GalI-MDCK cells and found that Gly407Ser was conserved with no additional sequence alterations, suggesting genetic stability of the NA mutant.

Finally, we performed molecular dynamics simulations for deciphering the mechanism of cross-RI displayed by Gly407Ser (Appendix). Our model suggests that Gly407Ser affects interaction networks involving a key arginine residue within the NA active site (Arg374) (*8*) and neighboring residues (Appendix Figure 2). In the wild-type protein, Arg374 forms hydrogen bonds with NAIs (Appendix Figure 2, panels A–C). There is a hydrogen bond between the Gly407 amine and the Arg374 carbonyl, and between the Trp408 amine and the Glu428 carbonyl, in addition to hydrophobic interactions between Trp408 and Val430 side chains. In the Gly407Ser variant, the orientation of Arg374 prevents hydrogen bond formation with NAIs (Appendix Figure 2, panels D–F). A hydrogen bond exists between the Ser407 amine and the Arg374 carbonyl and between the Ser407 side chain hydroxyl and the Glu428 carbonyl, in addition to hydrophobic interactions between the Trp408 and the Arg374 side chains.

In 2007, a Gly407Ser influenza B variant was recovered from a child after 3 days of oseltamivir therapy (*9*). That variant displayed 4- and 7-fold increases in oseltamivir and zanamivir IC_{50}levels, respectively, with an unexplained mechanism (*9*). Here, we identified a contemporary Gly407Ser influenza B variant in a patient before NAI therapy and propose a molecular mechanism for such a cross-RI phenotype. We cannot exclude nosocomial transmission of this virus despite evidence for some alteration in replication kinetics. The Gly407Ser mutation was detected in the absence of NAI constituting 100% of sequenced clones, did not affect NA activity, and was conserved after in vitro passages. Thus, such a variant may retain efficient transmissibility. Nevertheless, the effect of this mutation in a suitable animal model (ferrets) remains to be assessed. The potential for emergence of variants with cross-RI to available NAIs in the absence of treatment emphasizes the need for novel antiviral strategies (including combinations) against influenza B viruses.

This work was supported by a Canadian Institutes of Health Research (CIHR) foundation grant to G.B. (grant No. 229733) for a research program on the pathogenesis, treatment, and prevention of respiratory and herpes viruses.

About the Author

Dr. Abed is an associate professor at the Research Center of Infectious Diseases of the CHU de Québec-Laval University in Québec City, Quebec, Canada. His research interests include influenza A and B infections and mechanisms of antiviral resistance.

References

1. Samson M, Pizzorno A, Abed Y, Boivin G. Influenza virus resistance to neuraminidase inhibitors. Antiviral Res. 2013;98:174–85. http://dx.doi.org/10.1016/j.antiviral.2013.03.014
2. Abed Y, Boivin G. A review of clinical influenza A and B infections with reduced susceptibility to both oseltamivir and zanamivir. Open Forum Infect Dis. 2017;4:ofx105. http://dx.doi.org/10.1093/ofid/ofx105
3. Skowronski DM, Chambers C, De Serres G, Dickinson JA, Winter AL, Hickman R, et al. Early season co-circulation of influenza A(H3N2) and B(Yamagata): interim estimates of 2017/18 vaccine effectiveness, Canada, January 2018. Euro Surveill. 2018;23. http://dx.doi.org/10.2807/1560-7917.ES.2018.23.5.18-00035
4. WHO. Global monitoring of antiviral resistance in currently circulating human influenza viruses, November 2011. Wkly Epidemiol Rec. 2011;86:497–501.
5. Samson M, Abed Y, Desrochers FM, Hamilton S, Luttick A, Tucker SP, et al. Characterization of drug-resistant influenza virus A(H1N1) and A(H3N2) variants selected in vitro with laninamivir. Antimicrob Agents Chemother. 2014;58:5220–8. http://dx.doi.org/10.1128/AAC.03313-14
6. Marathe BM, Lévêque V, Klumpp K, Webster RG, Govorkova EA. Determination of neuraminidase kinetic constants using whole influenza virus preparations and correction for spectroscopic interference by a fluorogenic substrate. PLoS One. 2013;8:e71401. http://dx.doi.org/10.1371/journal.pone.0071401
7. Abed Y, Baz M, Boivin G. Impact of neuraminidase mutations conferring influenza resistance to neuraminidase inhibitors in the N1 and N2 genetic backgrounds. Antivir Ther. 2006;11:971–6.
8. Varghese JN, McKimm-Breschkin JL, Caldwell JB, Kortt AA, Colman PM. The structure of the complex between influenza virus neuraminidase and sialic acid, the viral receptor. Proteins. 1992;14:327–32. http://dx.doi.org/10.1002/prot.340140302
9. Hatakeyama S, Sugaya N, Ito M, Yamazaki M, Ichikawa M, Kimura K, et al. Emergence of influenza B viruses with reduced sensitivity to neuraminidase inhibitors. JAMA. 2007;297:1435–42. http://dx.doi.org/10.1001/jama.297.13.1435

Address for correspondence: Guy Boivin, CHU de Québec-Université Laval, CHUL, 2705 blvd Laurier, Sainte-Foy, RC-709, Quebec City, QC G1V 4G2, Canada; email: guy.boivin@crchul.ulaval.ca

Article DOI: https://doi.org/10.3201/eid2504.181554

Reduced Susceptibility to Neuraminidase Inhibitors in Influenza B Isolate, Canada

Appendix

Molecular Dynamics Simulations

Molecular dynamics simulations were performed for highlighting the mechanism of cross resistance displayed by the Gly407Ser mutation. A National Center for Biotechnology Information Protein Data Bank (NCBI PDB) BLAST (https://blast.ncbi.nlm.nih.gov/Blast.cgi) of the B/Quebec/1182C/2018 NA amino acid sequence identified B/Brisbane/60/2008 structure PDB IDs having the best sequence identity (94.8%), including 4CPL (uncomplexed NA), 4CPM (NA-oseltamivir), and 4CPN (NA-zanamivir). The amino acid sequence alignment was used to build a SWISS-MODEL (https://swissmodel.expasy.org/). Then, the WT and Gly407Ser systems were built using CHARMM-GUI (*1*) as previously described. Simulations were performed with the NAMD 2.12b1 (*2*) software using the CHARMM36m force field, TIP3P waters, a time step of 2 femtoseconds, and periodic boundary conditions. Nonbonded pair lists were updated at every step, and coordinates were saved every 2 picoseconds (ps) for analysis. Cutoffs for the short-range electrostatics and the Lennard-Jones interactions were 12 Å, with the latter smoothed via a switching function over the range of 10–12 Å. Long-range electrostatics were calculated via the particle mesh Ewald (PME) method, using a sixth-order interpolation and a grid spacing of ≈1 Å. Langevin damping with a coefficient of 1 ps–1 was used to maintain a constant temperature of 37°C, and the pressure was controlled by a Nosé-Hoover Langevin piston at 1 atm. The length of the bonds between hydrogens and heavy atoms were constrained using SETTLE for water molecules, and SHAKE for all other molecules. For each system, 3 trajectories of 150 nanoseconds (ns) were recorded, and the last 50 ns of each trajectory was used for analysis.

References

1. Jo S, Kim T, Iyer VG, Im W. CHARMM-GUI: a web-based graphical user interface for CHARMM. J Comput Chem. 2008;29:1859–65. http://dx.doi.org/10.1002/jcc.20945

2. Phillips JC, Braun R, Wang W, Gumbart J, Tajkhorshid E, Villa E, et al. Scalable molecular dynamics with NAMD. J Comput Chem. 2005;26:1781–802. http://dx.doi.org/10.1002/jcc.20289

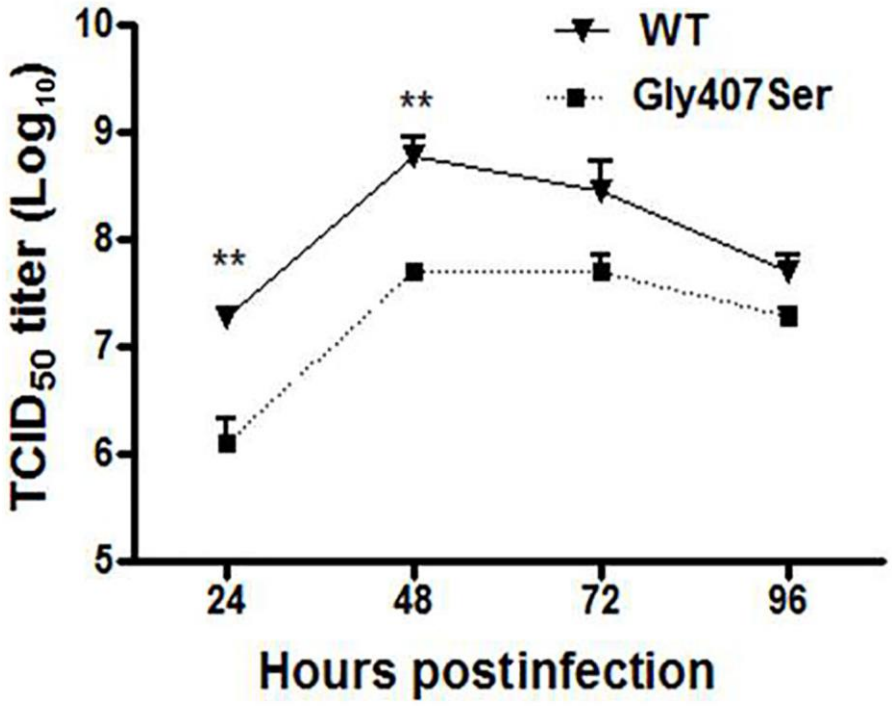

Appendix Figure 1. Replicative properties of influenza B isolates in vitro. Confluent ST6GalI-MDCK cells were infected with the WT and Gly407Ser influenza B isolates at a multiplicity of infection (MOI) of 0.001 PFU/cell. Supernatants were harvested at the indicated times and titrated by $TCID_{50}$ assays. Mean viral titers of triplicate $\pm$SD are shown. ** $p < 0.01$.

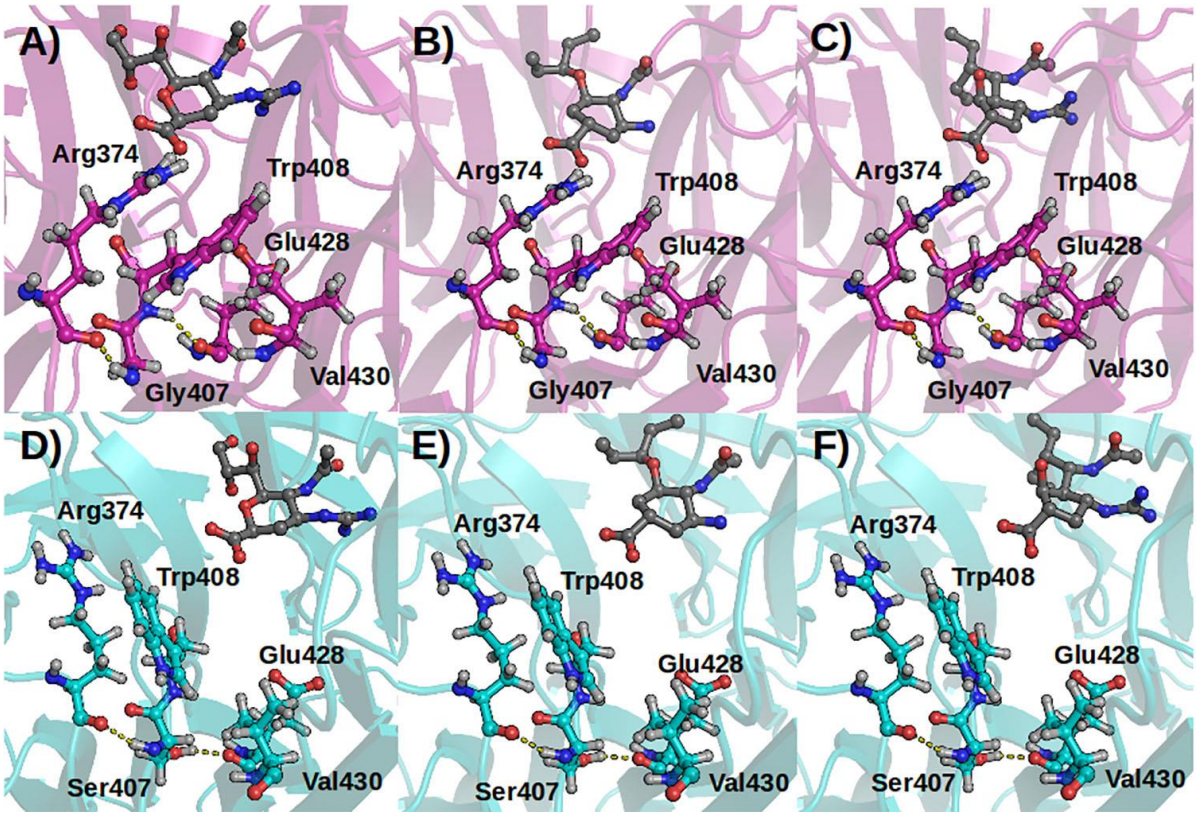

Appendix Figure 2. Trajectory analysis and molecular dynamics simulations of the Gly407Ser variant. Typical structures of the WT (in pink) and the Gly407Ser variant (in cyan). The residues involved in the structural changes from the Gly407Ser mutations are in sticks and spheres. The molecules of zanamivir (A and D), oseltamivir (B and E), and peramivir (C and F) were included to illustrate the potential interactions with Arg374. The molecules, represented with gray sticks and spheres, were positioned according to a structural alignment of the PDB 4CPN (PMID 24795482) to both the WT and the Gly407Ser variant. For the Gly407Ser variant, Arg374 is locked in an orientation that prevents hydrogen bond formation with NAIs.